RSC Advances

ROYAL SOCIETY OF CHEMISTRY

www.rsc.org/advances

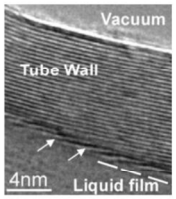

364x186mm (96 x 96 DPI)

Variations of the interlayer spacing in carbon nanotubes.

Oxana V. Kharissova, Boris I. Kharisov*
Universidad Autónoma de Nuevo León, Monterrey, México.
E-mail bkhariss@hotmail.com

Abstract

The analysis of earlier classic and recent reports on the interlayer distances in MWCNTs is given in this review. Simulations on interlayer spacing, applications of Raman spectroscopy, X-ray and neutron diffraction methods, influence of synthesis methods, heat and radiation (gamma-rays, electron and ion beams) treatments are discussed, as well polygonization and intercalation of CNTs. It is shown that the spacing values for DWCNTs and MWCNTs vary from 0.27 up to 0.42 nm. The most common values are in the range 0.32÷0.35 nm and do not strongly depend on the synthesis method. Diameter of CNTs and symmetry of layers do influence on the interwall spacing.

Keywords: carbon nanotubes, interlayer distance, synthesis method, calculations.

Introduction

Famous objects in the nanotechnology, the carbon nanotubes (CNTs),[1] [2] among other carbon allotropes,[3] seem to be very good studied after publication of thousands of experimental articles, reviews, books and chapters. Such important property of multi-wall CNTs (MWCNTs), as interlayer distance/spacing was determined much time ago,[4] [5] in particular in earlier nice classic works of Dresselhaus,[6] who observed that the interlayer distance ranges from 0.342 to 0.375 nm, and that it is a function of the curvature and number of layers/shells comprising the tube. However, in the last 15 years several reports have appeared periodically, sometimes in contradiction between them, on slight variations between interlayer distances. We believe that this topic has not yet lost its importance due to simple reason that the carbon nanotubes possess enormous applications, where properties of their nanocomposites and nanomaterials could depend on interspacing distances. In this short review, we present a generalization of reports during this period, paying attention to the main reasons for interlayer spacing variations.

Classic definitions

According to classic knowledge, the CNTs form two structurally distinct classes. The first to be discovered, multi-wall CNTs (MWNTs), exhibit, in particular, a Russian doll-like structure of nested concentric tubes.[7] The interlayer spacing in 3D-crystalline graphite is 0.335 nm, suggesting a similarly weak interaction between individual shells in MWNTs (Fig. 1).[8] When a nanotube contains only two layers, it is referenced as double-walled carbon nanotube (DWNT). Interlayer spacing of DWNTs is also not a constant, ranging from 0.34 nm to 0.41 nm.[9] Mechanical properties of CNTs are closely related to those of graphite. The outer diameter in MWCNTs is starting from 2.5 nm, while for single-wall CNTs (SWCNTs) this value ranging from 0.6 to 2.4 nm.[10] [11] Stiff sp^2-

* *Corresponding author*. E-mail bkhariss@hotmail.com.

hybridized in-plane σ-bonds, 1.42 Å long, give them an exceptionally high Young's modulus while out-of-plane π-bonds, responsible for the main features of the electronic properties, govern the weak van der Waals interlayer cohesion. Different shells of MWNTs interact through van der Waals interaction (in the absence of structural defects) while SWNTs form bundles in which the intertube coupling is also determined by the van der Waals interaction. The combination of strong sp^2 bonding and weak van der Waals interaction in these structures lies at the origin of the exceptionally diverse mechanical behavior of nanotubes.

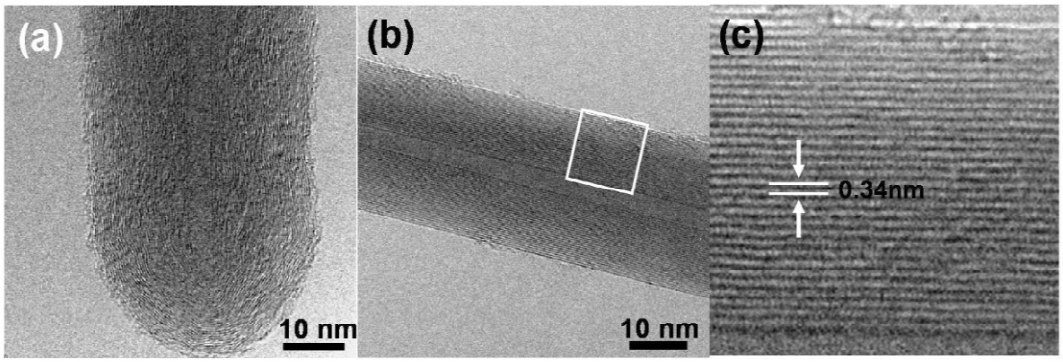

Fig. 1. (a) HR-TEM image of highly disordered carbon nanotubes; (b) HR-TEM image of annealed carbon nanotube at 2800°C showing linear, stiff graphene layers along the tube axis; (c) enlarged HR-TEM image of (b). Note that 0.34 nm is the distance between adjacent graphene layers.

In the works of Dresselhaus,[12 13] variations in the inter-shell spacing were studied, showing that all studied tube diameters had the inter-shell spacing (d_{002}) ranges from 0.33 to 0.39 nm, and that (d_{002}) increases as the tube diameter decreases. The simple elastic constant model implies an epitaxy-like growing mechanism for carbon nanotubes. Upon forming the first cylinder of a graphene sheet, the diameter of the second cylinder is determined by the energetic equilibrium between the two graphene shells. This process continues until the curvature of the graphene shells become negligible, so that the elastic energies play less important roles.

Simulations / DFT calculations on interlayer distances

Major part of simulation studies on interlayer spacing in carbon nanotubes have been carried out using DWCNTs as a model.[14 15] In particular, it was indicated that the stability of a DWNT depends only on the interlayer spacing, which reaches an energy minimum when the mean interlayer separation equals 0.34 nm, independent of the chiralities of the two constituent tubes.[16] Atomistic simulations were performed to investigate the torsional behavior of abnormal DWCNTs (Fig. 2) with an interlayer distance of less than 0.34 nm (Table 1) and carbon nanowires (CNWs) made of linear carbon-atom chain (C-chain) encapsulated inside single-walled carbon nanotubes (SWCNTs) subject to torsional motion.[17] These simulations indicated that the effect of the van der Waals (vdW) interaction is more significant for abnormal DWCNTs than for normal DWCNTs. The critical torsional moments of abnormal DWCNTs are considerably enhanced compared with those of corresponding normal DWCNTs. It is worth noting that the critical torsional moment does not always increase with a decrease in the interlayer distance of DWCNTs.

Table 1. Parameters of three DWCNTs.

DWCNTs	Inner tube radius (nm)	Outer tube radius (nm)	Interlayer distance (nm)
((4, 0), (13, 0))	0.157	0.509	0.352
((5, 0), (13, 0))	0.196	0.509	0.313
((6, 0), (13, 0))	0.235	0.509	0.274

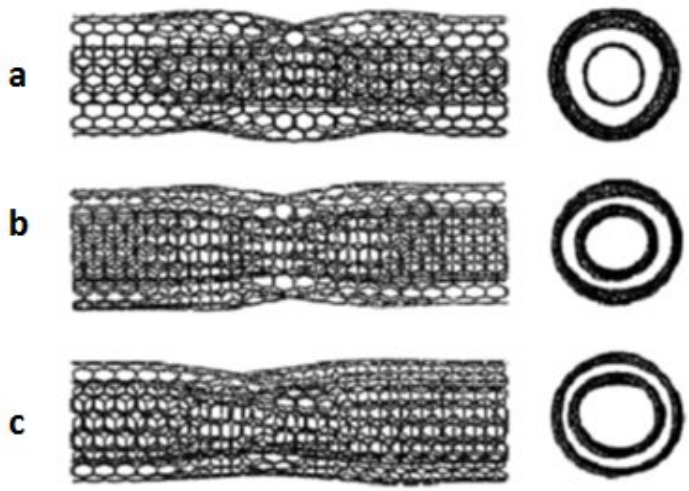

Fig. 2. The primary buckling morphologies of DWCNTs: (*a*) ((5, 5), (10, 10)) DWCNT; (*b*) ((6,6), (10,10)) DWCNT and (*c*) ((7, 7), (10, 10)) DWCNT.

Equilibrium structures of DWNT, as well as the interwall interaction energies of DWNT, were computed using a local density approximation within DFT theory with periodic boundary conditions and Gaussian-type orbitals.[18] The interwall distances d, translational lengths t_d of the unit cell, the relative differences $t_\delta = (t_s^2 - t_s^1)/t_d$, and Young's moduli E_d of DWNT are presented in Table 2. For the armchair (n, n)@(n+5, n+5) and zigzag (9, 0)@(18, 0) DWNT, the interwall distance is close to the interlayer separation in graphite and the calculated values of the energy U_{int} are comparable with the interwall interaction energy of 35–40 meV/atom obtained with the Lennard-Jones potential and experimental value of the interlayer interaction in graphite.

Table 2. Structural characteristics, elastic properties, and interwall interaction of DWNT: d (in Å) is the interwall distance, t_d (in Å) and E_d (in TPa) are the translational length of the unit cell and Young's modulus, the parameter t_δ determines the difference in translational lengths of DWNT and constituent SWNT, and U_{int} (in meV/atom) is the interwall interaction energy (per one atom of the outer wall) of DWNT.

Nanotube	d, Å	t_d	t_δ	E_d	U_{int}
(4,4)@(10,10)	4.011	2.4444	0.00317	0.992±0.002	13.29
(5,5)@(11,11)	4.017	2.4424	0.00061	0.989±0.003	13.36
(6,6)@(12,12)	4.021	2.4421	0.00020	1.005±0.003	13.67
(5,5)@(10,10)	3.344	2.4425	0.00058	1.085±0.004	23.83
(6,6)@(11,11)	3.350	2.4421	0.00019	1.106±0.003	24.09

(7,7)@(12,12)	3.353	2.4421	0.00013	1.106±0.003	24.60
(9,0)@(18,0)	3.478	4.2315	0.00116	1.049±0.003	24.26
(10,0)@(20,0)	3.875	4.2305	0.00091	1.016±0.002	16.76

Large-scale quasi-continuum simulations were performed to determine the stable cross-sectional configurations of free-standing MWCNTs {armchair (AC), zigzag (ZG), and chiral (CH) MWCNTs} (Figs. 3 and 4).[19] It was shown that at an interwall spacing larger than the equilibrium distance set by the interwall van der Waals (vdW) interactions, the initial circular cross-sections of the MWCNTs are transformed into symmetric polygonal shapes or asymmetric water-drop-like shapes. The simulations also showed that removing several innermost walls causes even more drastic cross-sectional polygonization of the MWCNTs. It was also shown that the symmetry of the layers of the multi-wall tubes strongly affects the interwall interaction.[20] The strongest interaction was found for the commensurate tubes with achiral walls. On the other side, the tubes with chiral walls interact negligibly.

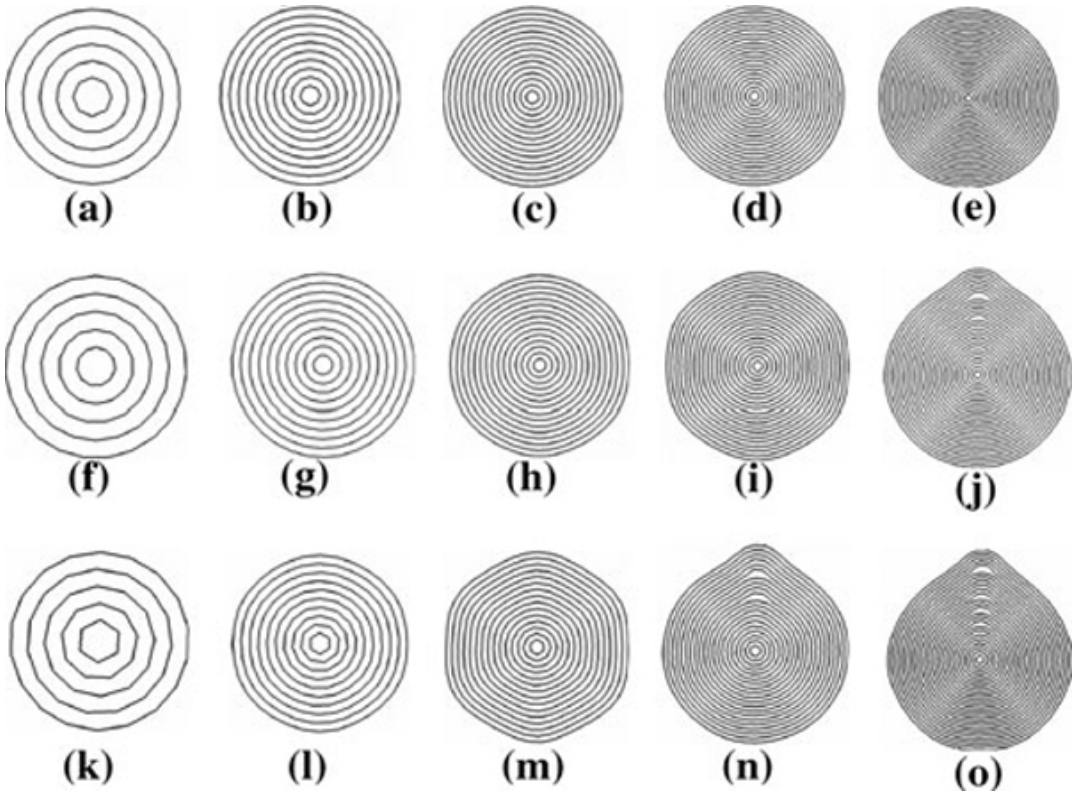

Fig. 3. Cross-sectional views of relaxed MWCNTs. From left to right on each row, the wall numbers are 5, 10, 15, 20, and 25. Top AC MWCNTs; middle ZG MWCNTs; bottom CH MWCNTs.

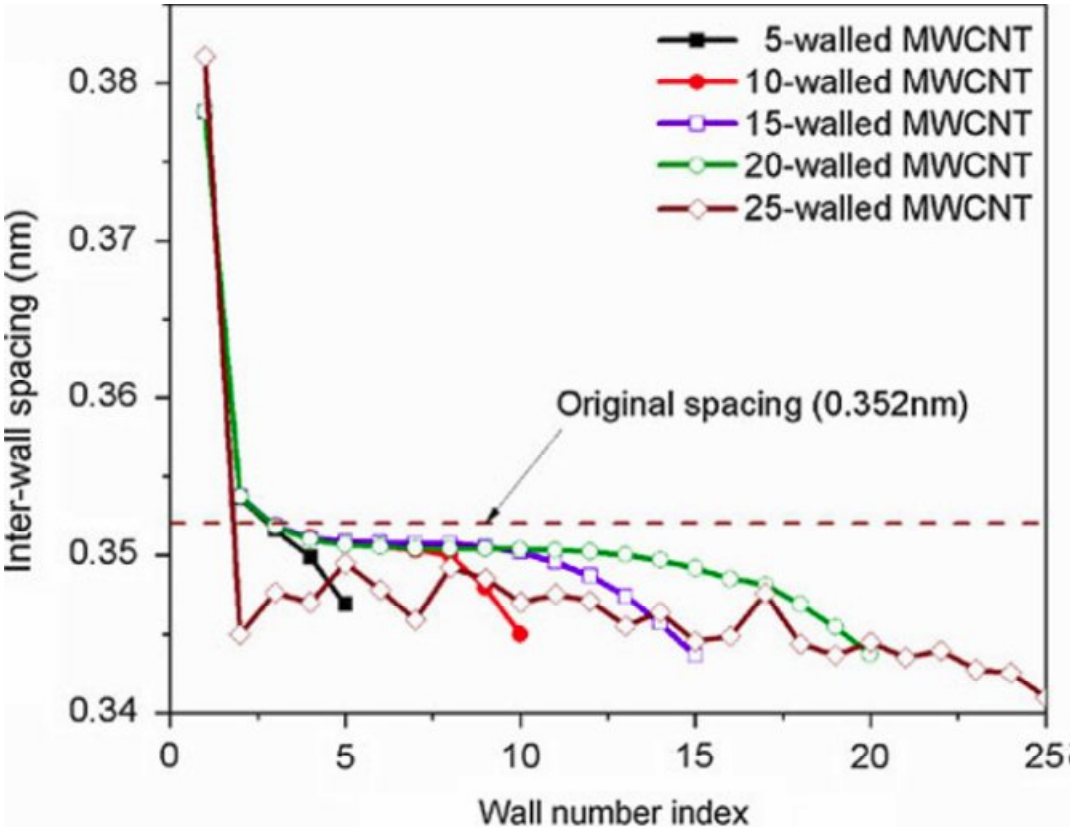

Fig. 4. The inter-wall spacing of the relaxed ZG MWCNTs shown in the previous Figure {from (f) to (j)}.

The effect of intertube van der Waals interaction on the stability of pristine and covalently functionalized CNTs under axial compression was investigated,[21] using molecular mechanics simulations. After regulating the number of inner layers of the armchair four-wall (5, 5)@(10, 10)@(15, 15)@(20, 20) and zigzag four-wall (6, 0)@(15, 0)@(24, 0)@(33, 0) carbon nanotubes, the critical buckling strains of the corresponding tubes were calculated. It was emphasized that the equilibrium interlayer space is 0.337 nm and 0.350 nm for the pristine armchair and zigzag tubes, respectively[22], due to the different chirality structures. The equilibrium space for any two graphene layers is 0.34 nm. Therefore, there exists an intertube vdW repulsive interaction in the armchair multi-wall tubes and an intertube attractive interaction in the zigzag multi-wall tubes, even when no compression strain is applied. As compression strain is applied, both the Poisson effect and the domino effect, resulting from the collapse, contribute to the repulsive interaction, which greatly enhances the stability of the armchair tubes. However, the intertube repulsive interaction occurs only until the intertube space becomes smaller than 0.34 nm. Among zigzag tubes, the deviation by 0.01 nm in intertube space needs to be compensated by means of the Poisson effect and the collapse of the outermost tube.

Simulation studies on CNTs can lead to unusual applications. Thus, DFT calculations of the interaction between nanotube walls were carried out and, on their basis, a new concept was proposed for an electromechanical nanothermometer.[23] The energy U of the interaction between two neighboring walls of a DWCNT depends on the coordinates describing the relative position of the walls: the angle φ of relative rotation of the walls about the nanotube axis and the relative displacement z of the walls with respect to this

axis. It was demonstrated that the nanothermometer can be used for measuring the temperature in spatially localized regions with sizes of several hundred nanometers. Since the measurement of the temperature by the nanothermometer under consideration is based on the measurement of the conductivity, the nanothermometer can be calibrated using a thermocouple.

Studies by other methods

Classic Raman spectra studies were performed on the DWNTs at different E_{laser} of excitation.[24] The interlayer distance of the DWNTs calculated from radial breathing mode (RBM) was found to be varied from 0.335 to 0.42 nm. Also, a systematic study[25] on the diameter dependent spectral features in X-ray diffraction (XRD) and Raman scattering studies of MWCNTs of various diameters in the range 5−100 nm was carried out. HRTEM imaging revealed a systematic decrease in the interwall separation from 3.8 Å down to 3.2 Å as the diameter of nanotubes increases from 5.8 nm to 63.2 nm (Fig. 5). Analysis of the XRD patterns showed an exponential decrease in d_{002} interlayer spacing with increasing tube diameter, in close agreement with the HRTEM results. The authors believed that the increase in intershell spacing with decreased nanotube diameter results primarily from the high curvature and associated strain in the lower diameter nanotubes. It is likely that high strain in the low diameter tubes causes structural defects in the nanotube walls that may be charged and it causes coulombic repulsion between the tube walls with charges of the same sign. This would result in a higher d-spacing for the low diameter tubes. On the other hand, in a large diameter MWCNT the interaction among the walls increases with the increase in the number of walls and as a result the interwall separation may decrease, as observed experimentally. In addition, in a recent report,[26] for raw CNTs, without any admixtures and carbon deposits, average distance between graphene layers (d_{002}) was calculated as follows. Position of the (002) band is connected with an average distance between graphene layers (d_{002}) and can be described as: $d_{002} = \lambda / 2\sin\theta_{002}$, where λ the wavelength of the X-ray radiation, θ is the Bragg angle of the graphite (002) peak. An average distance between graphene layers was found to be 3.52 Å. An average XRD result was similar, but slightly higher (3.62 Å). Indeed, after electronic microscopy methods, X-ray and neutron diffraction measurements of CNTs are classic instrumental techniques to study interlayer spacing variations in CNTs.[27]

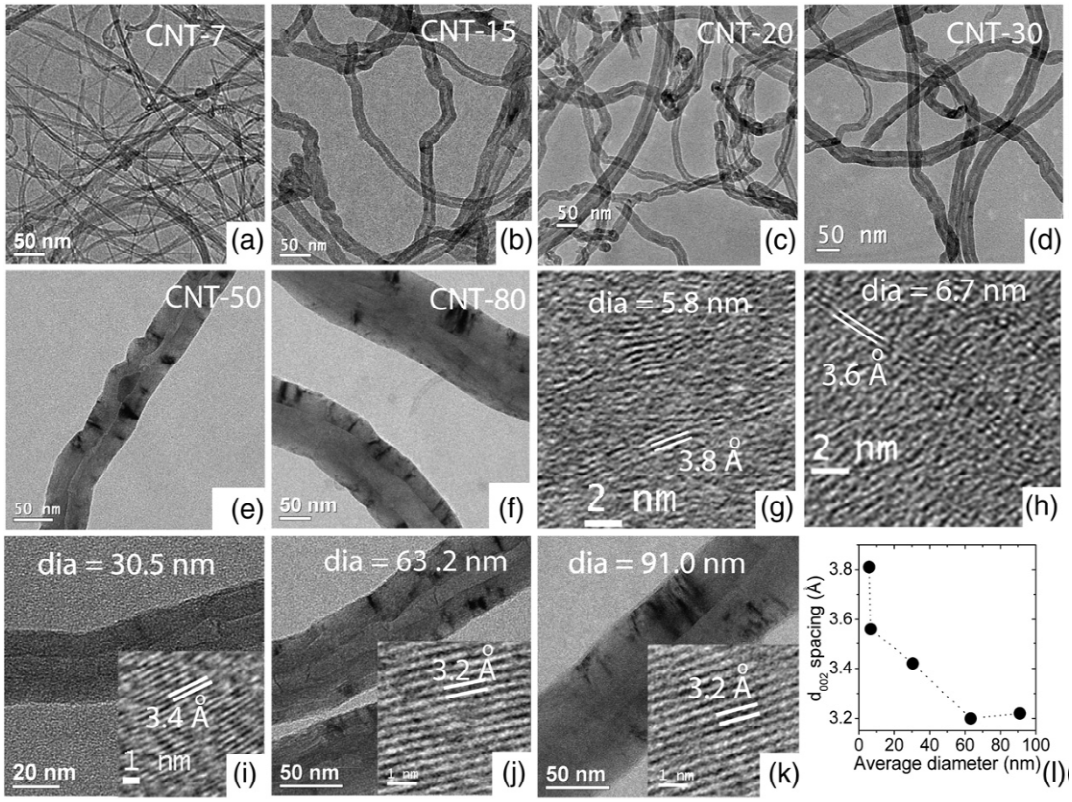

Fig. 5. HRTEM images of various diameter MWCNTs (a) CNT-7, (b) CNT-15, (c) CNT-20, (d) CNT-30, (e) CNT-50 and (f) CNT-80. Systematic decrease in d_{002} lattice spacingwith increasing diameter (D): (g) d_{002}=3.8 Å, D=5.8 nm, (h) d_{002}=3.6 Å, D=6.7 nm (i) d_{002}=3.4, D=30.5 nm, (j) d_{002}=3.2 Å, D=63.2 nm, (k) d_{002}=3.2 Å, D=91 nm. Insets in (i–k) show the HRTEM lattice images of the corresponding nanotubes. (l) Variation of d_{002} lattice spacing with diameter of MWCNTs as measured from HRTEM images.

Influence of synthesis method

CVD and microwave plasma-enhanced CVD. The combined growth process of CNTs and few-layer graphene sheets (FLGS) by means of microwave plasma-enhanced chemical vapor deposition was described.[28] During the experiment, each position on the samples was exposed to a specific carbon radical concentration. This value was found to be the most important parameter for determining the morphology of the as grown carbon nanostructures, either tubular CNTs or plain FLGS. It was shown (Fig. 6) that the flakes on the average consists of 13 atomic layers graphene, since the measured interlayer distance (0.32 nm) corresponds to the tabulated values for graphite. Nickel particles only catalyze the growth of CNTs if the carbon radical concentration is low. A rapid transformation of morphology from tubes to flakes was observed when the carbon radical concentration increased. The flakes, formed at the highest carbon radical concentration, were identified as FLGS, only a few atomic graphene layers thick but up to several micrometers wide. According to an earlier report,[29] the results of CVD-synthesized MWCNTs indicated that interwall coupling in MWNT's is rather weak compared with its parent form, graphite, so that one can treat a MWNT as a few decoupled 2D single-wall tubules. The thermal conductivity was found to be low,

indicating the existence of substantial amounts of defects in the MWNT's prepared by a CVD method. Two facts may be responsible for the weak interwall coupling: the larger interwall distance in MWNT's than the interlayer distance in graphite, and the turbostratic stacking of adjacent walls which is unavoidable in the rolled-up structures. The interwall distance decreases as a tubule's diameter increases. At diameters >10 nm it saturates to ~0.344 nm, a characteristic interlayer distance in turbostratic stacking. Therefore, the weak interwall coupling in MWNT's is rather caused by the turbostratic stacking of adjacent walls.

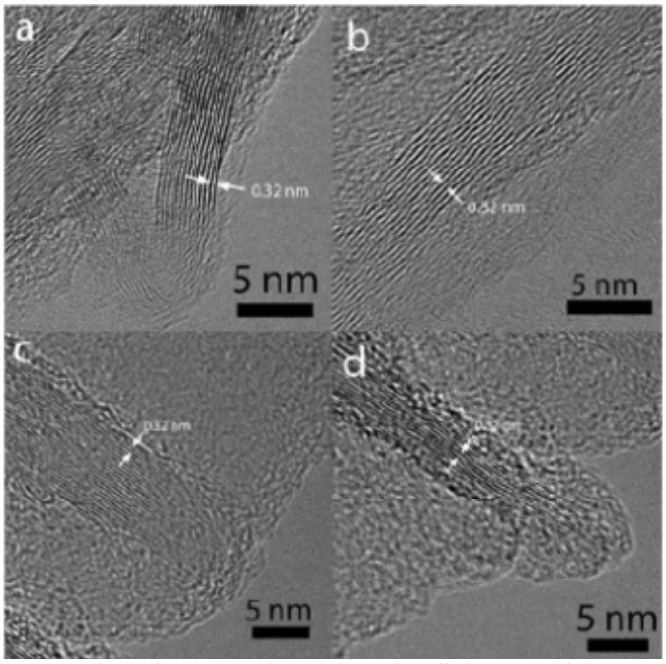

Fig. 6. TEM micrographs of FLGS show that the flakes on the average consist of 13 atomic layers with a typical interlayer distance of graphite.

Pyrolysis. The unbroken twisted nanotubes, obtained by pyrolysis of sugar water, had atomic interlayer distance of ~0.36 nm (Fig. 7).[30] Some of these nanotubes were found to be approximately 10 μm long. This length is longer than the length of graphene wall nanotubes fabricated by other pyrolytic template methods.

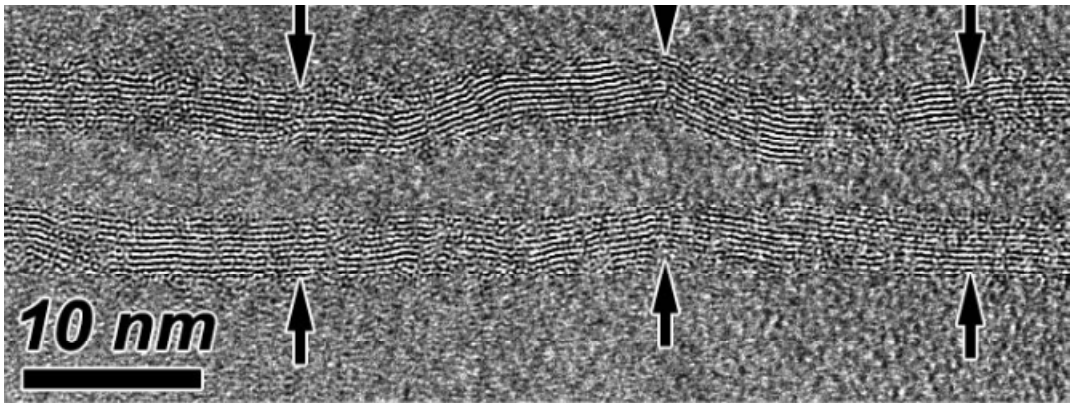

Fig. 7. A high resolution TEM image of the carbon nanotube region.

Hydrothermal synthesis and influence of intercalation.[31] Graphitic carbon nanotubes, synthesized hydrothermally by using an ethylene glycol ($C_2H_4O_2$) solution in the presence of a Ni catalyst at 730–800°C under 60–100 MPa pressure, were found to have high perfection of graphene layers, long and wide internal channels and Ni inclusions in the tips.[32] In some their locations, uniform swelling and *intercalation* of tube walls resulting in almost doubling of the lattice spacing (Fig. 8) were observed (for details on the intercalation of CNTs, see[33 34]). The observed interplanar spacing of 0.61 nm is in agreement with the 0.6–0.7 nm spacing in GO (a similar intercalation of multiwall nanotubes resulting in the increase of the lattice spacing up to 0.95 nm was achieved using $FeCl_3$[35]). The authors noted that an explanation for the increased spacing may be due to penetration of a monolayer of water molecules between graphene sheets. During growth of a tube, the synthesis fluid, which is a supercritical mixture of CO, CO_2, H_2O, H_2, and CH_4, enters the tube. After closure of the tube and temperature decrease, aqueous liquid and gases are trapped inside. Therefore, closed hydrothermal nanotubes, unlike conventional nanotubes produced in vacuum or at ambient pressure, contain water and gases encapsulated under pressure. Considering that the size of oxygen governs that of a water molecule (about 0.3 nm), the spacing increase due to water penetration should be 0.335+0.3 nm = 0.635 nm. This value is comparable with the one measured by authors. In addition, the temperature increase results in a chemical reaction between the tube and the supercritical fluid and dissolution of carbon. This reaction leads to dissolution of the carbon wall (Fig. 9) in the area of the inclusion and, ultimately, puncture of the tube wall and loss of the tube fluid to the microscope environment.

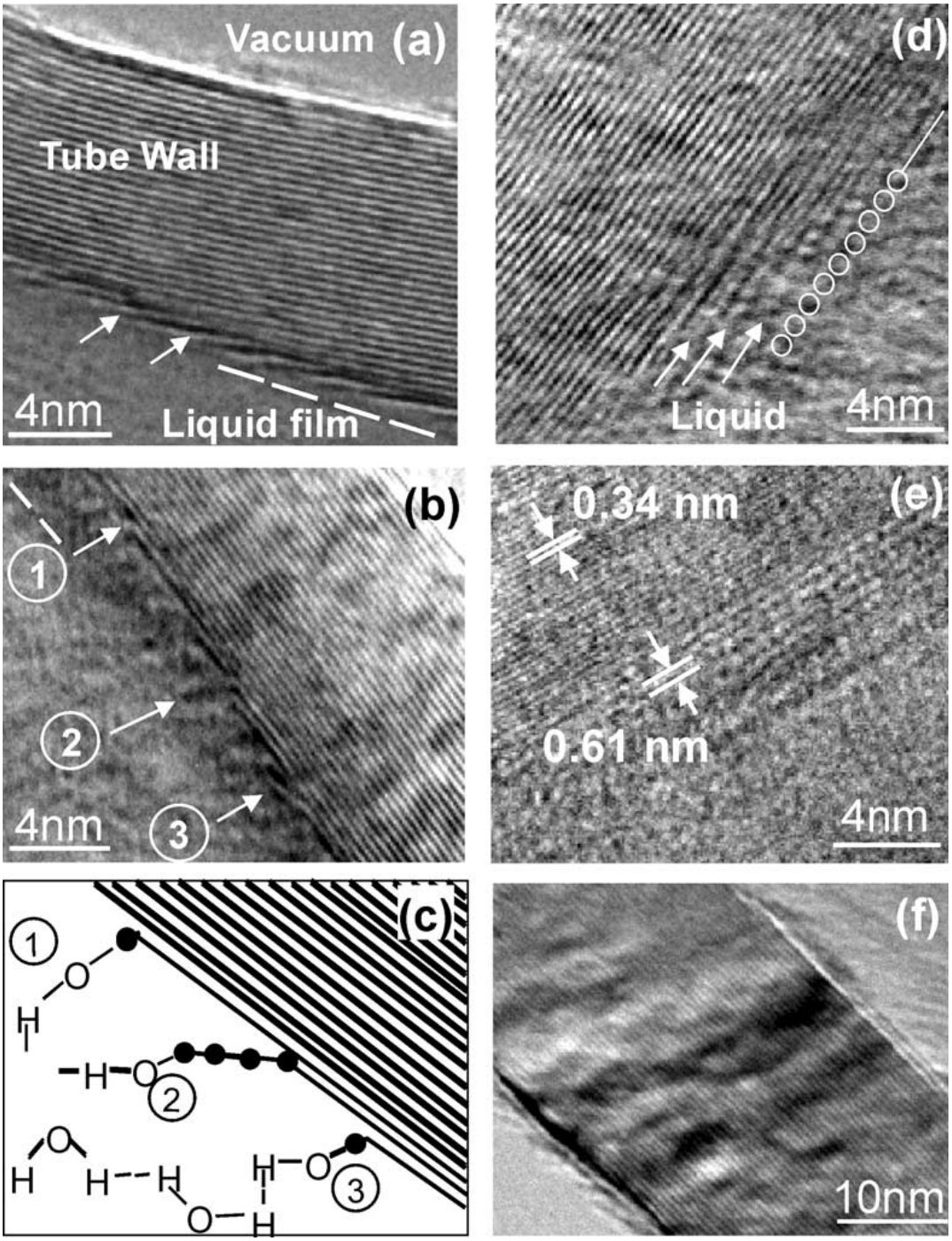

Fig. 8. Lattice fringe images of the tube wall in the vicinity of a liquid/gas interface showing the structural changes in the graphite layers in contact with the liquid: (a) penetration of the liquid between the layers in the presence of a thin (~1 nm) liquid layer covering the inner surface of the tube; (b) a thicker (~2 nm) liquid layer – radial contraction of the edges of the innermost carbon cylinders is clearly seen in both micrographs; (c) schematic showing interaction of terminated graphene edges with water; (d) strong interaction leading to dissolution of hydrated carbon layers; (e) intercalation of inner layers of the nanotube; (f) dry open tube that does not show any carbon-edge bending behavior.

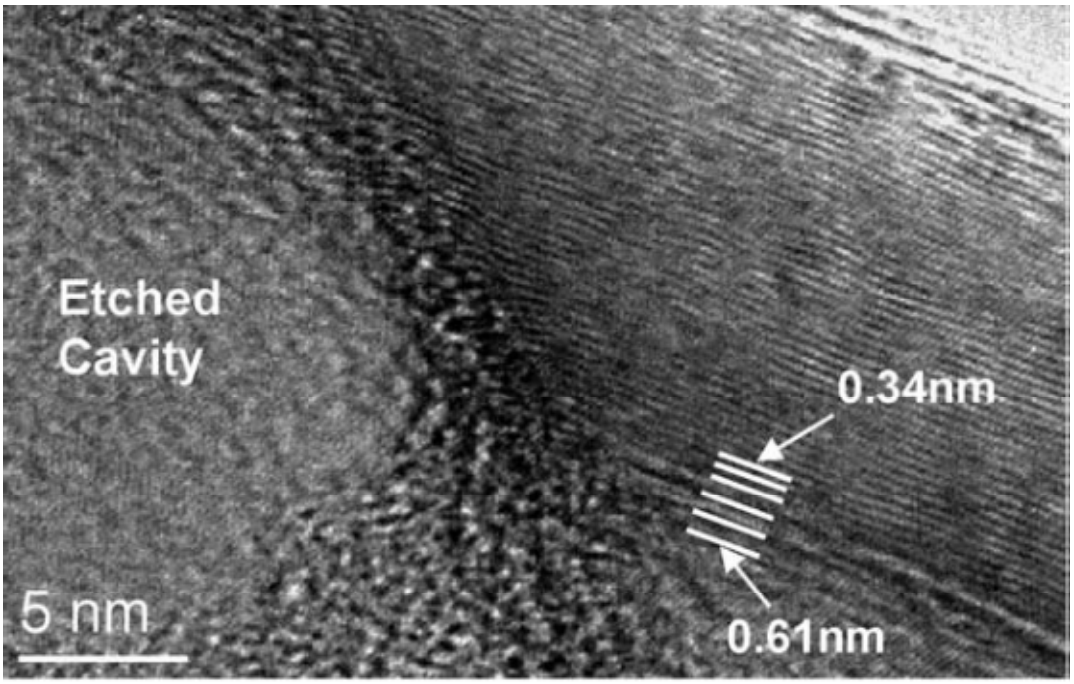

Fig. 9. TEM micrograph of a nanotube with a partially dissolved wall.

Comparison of various methods (the case of interlayer distances between different DWCNTs in their bundles). The DWNTs can be synthesized by different methods such as electric arc discharge, coalescence of C_{60} peapods, and catalytic chemical vapor deposition (CCVD) using supported or floating catalysts (see[36] and references therein). Depending of these synthesis methods, different values of the intertube spacing have been reported. Large and isolated DWNTs produced by electric arc discharge presented an interlayer spacing of 0.39 nm, a value larger than that usually observed for MWNTs (0.34 nm). A similar value, 0.36 nm, was found for DWNTs synthesized by coalescence of C_{60} peapods. Using the CCVD method, the interlayer spacing observed was in the range of 0.34 to 0.41 nm.

Influence of heat and irradiation treatments

It was shown[37] experimentally that *polygonization* (Fig. 10) of multi-walled carbon nanotubes or nanofibers can be induced at sufficiently high *heat-treatment temperatures* and with sufficiently large diameters. One central finding was the stabilization of polygonal shapes at high temperatures by the configuration entropy associated with the creation of the Stone-Wales defects. As a consequence of the polygonization, the interlayer spacing of the MWPNTs contracts to a value distinctly smaller than the established graphene interlayer spacing. The graphene interlayer spacing in multi-walled carbon nanofibers heat treated above ≥2800 K is distinctly smaller than d_{min} in graphite (0.3354 nm) (Fig. 11). In a related report,[38] thermal expansion of MWCNTs after high-temperature heating (HTT) at 3173K under a pure argon flow was described, suggesting and confirming that for the as-grown nested MWNTs with high defects, polygonization is preferred for MWNTs greater than 50 nm, while scrolllike structure is recommendable for MWNTs in diameters less than 50 nm, after heat treatment. XRD-based data on interwall spacing showed that the d_{002} values (in Å) decrease after HTT as

follows: a) average diameter of MWCNTs 10 nm (3.476→3.425), 50 nm (3.477→3.393), 70 nm (3.478→3.391), and 100 nm (3.480→3.385).

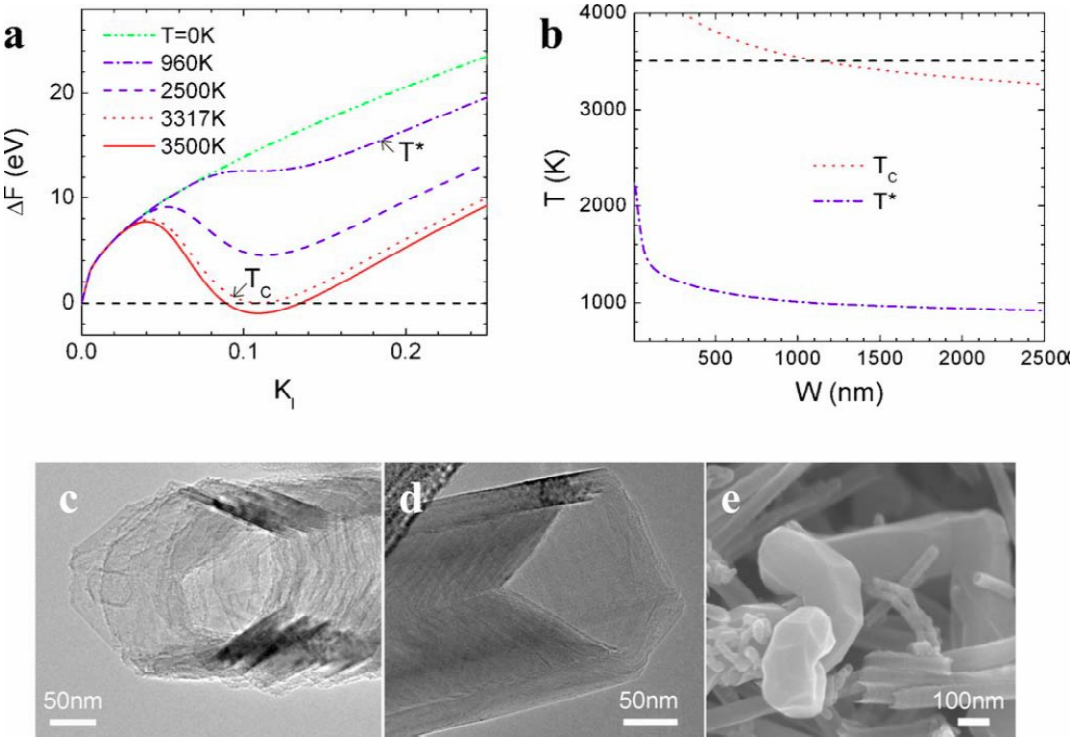

Fig. 10. a) Total free energy of single-wall polygonal nanotubes per unit length relative to that of the conventional (or circular) carbon nanotubes as a function of the local curvature at the tube circumference W=2000 nm. b) Dependence of the two critical temperatures on W. TEM images [c) and d)] and SEM image e) confirm the polygonization of the nanotubes upon high-temperature heat treatment (T≥2800 K).

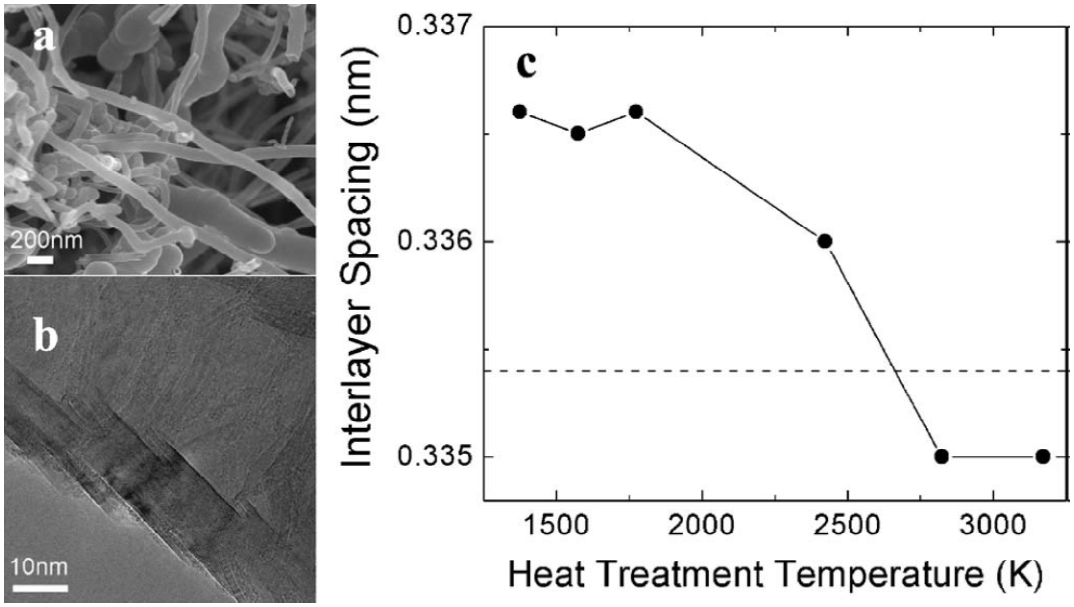

Fig. 11. SEM a) or TEM b) image showing that as-grown fibers have circular cross sections a) and heat-treated fibers are well graphitized b). c) Experimentally measured interlayer spacing of the fibers as a function of the heating temperature.[39] The dotted line marks the spacing of natural graphite. The error bar is within $4x10^{-5}$ nm, smaller than the size of the data points.

Irradiation of MWCNTs with the 800-keV *electron beam* of a TEM microscope was shown to induce anisotropic collapse of the nanotube.[40] Tight-binding molecular-dynamics simulations of tube response following momentum transfer from large-angle electron-nuclear collisions revealed a strongly anisotropic threshold for atomic displacement. The electron beam preferentially damages the front and back of the nanotube, producing the observed anisotropic collapse perpendicular to the direction of the beam. Collapse accelerates as the graphitic interwall distance of 0.34 nm is approached. Collapse in one portion increases the van der Waals and residual covalent attraction between the nearby opposing sections of inner wall, possibly inducing a zipper-like closure of the damaged nanotube reminiscent of that anticipated for a mechanically flattened nanotube. In case of *gamma-rays*, MWCNTs were irradiated by γ-rays in air and epoxy chloropropane (ECP) with an absorbed dose 200 kGy.[41] It was found that MWCNTs showed an opposite behavior in structural change when irradiated in the two different media. γ-Ray irradiation *decreased* the interwall distance of MWCNTs {from 3.44 to 3.42 Å (6%)} and improved their graphitic order in air, while irradiation in ECP *increased* the interwall distance (from 3.44 to 3.47 Å) of MWCNTs and disordered the structure. The authors explained that γ-rays caused the improvement in graphitic order of graphite and carbon fibers in air and damaged and shortened the nanotube structure in polar liquid. Due to great penetrating power of γ-rays, MWCNTs irradiated in air show a significant rearrangement and the defect concentration can be decreased. As a result, the interwall spacing decreases because the defective graphenes typically have large interlayer spacing. Another possible mechanism is that the irradiation can push one carbon atom out of the graphene plane and then a cross-link between neighboring graphene layers is formed. However, besides the above changes, γ-ray irradiation in ECP can shorten tubes, and ECP might be strongly bonded to dangling bonds of tubes to form grafting chains. The distance of graphene in MWCNTs increases, as the defective structure increases. For the case of *ion irradiation*, the irradiation of a bundle of nanotubes by 100, 250, 500, 750 and 1000 eV Ar ions was simulated.[42] It was indicated that the most common defects produced at all energies are vacancies on nanotube walls. The vacancies are metastable and can transform to other defect by saturating dangling bonds and deforming the carbon network of nanotubes. The spatial distribution of the defects proved to be highly non-uniform and has several maxima. These maxima are located in the interface regions between nanotubes in different layers, where the atomic density is the highest. It was also demonstrated that ion irradiation gives rise to the formation of intertube covalent bonds mediated by carbon recoils and nanotube lattice distortions due to dangling bond saturation. The number of inter-tube links, as well as the overall damage, linearly grows with the energy of incident ions. In case of chemical modification/functionalization of CNTs surface, for instance with fluorine atoms,[43 44] the interwall spacing of the MWCNT was found to be larger than in unfluorinated areas.

Conclusions

As it is seen from classic reports of 1999-2001 and more recent publications, variations in interlayer/intershell distances (between adjacent graphene layers), from 0.27 to 0.42 nm, have been observed for DWCNTs and MWCNTs. The most common values are in the range 0.32÷0.35 nm and do not strongly depend on the synthesis method. Diameter of CNTs and symmetry of layers do influence the interwall spacing. The interlayer distances could vary upon external treatments (*i.e.*, irradiation or functionalization) and depend on the media (for instance, in air or organic medium). Electronic properties of CNTs can be affected by variation of interwall spacing. Heat-treatment polygonization of CNTs also influences interwall spacing,[45] [46] [47] as well as intercalation. Unusual applications could appear applying calculations of the interaction between nanotube walls, for instance, a new concept, proposed for an electromechanical nanothermometer. It should be also emphasized that errors in measurements of interwall spacing by various methods (TEM, XRD, etc.) are significant and can be a reason for variation in the reported data.

At last, discussing the interlayer spacing in CNTs and graphite, we need to mention also the hexagonal boron nitride, which was recently underlined and has a similarity with the structures above. Specifically, the electrostatic attractions between the oppositely charged atomic centers in adjacent h-BN layers are expected to result in a considerably shorter interlayer distance than that measured for graphite.[48] Nevertheless, the interlayer distances in graphite (3.33−3.35 Å) and h-BN (3.30−3.33 Å) are essentially the same, suggesting that electrostatic interactions between partially charged atomic centers, which exist in h-BN and are absent in graphite, have little effect on the interlayer binding. This is consistent with the fact that van der Waals (vdW) forces are responsible for anchoring the h-BN layers at the appropriate interlayer distance, rather than electrostatic interactions.

Acknowledgement

The authors are very grateful to Prof. *Yuri Gogotsi* (Drexel University) for critical revision of this manuscript and highly valuable suggestions.

References

[1] Monthioux, M.; Kuznetsov, V.L. Guest Editorial: Who should be given the credit for the discovery of carbon nanotubes? *Carbon*, **2006**, *44*, 1621 http://nanotube.msu.edu/HSS/2006/1/2006-1.pdf.

[2] Gogotsi, Yu. How safe are nanotubes and other nanofilaments? *Mat. Res. Innovat.*, **2003**, *7*, 192-194.

[3] Gogotsi, Yu.; Libera, J.A.; Kalashnikov, N.; Yoshimura, M. Graphite Polyhedral Crystals. *Science*, **2000**, *290*, 317-320.

[4] Qian, D.; Wagner, G.J.; Kam Liu, W.; Yu, M.F.; Ruoff, R.S. Mechanics of carbon nanotubes. *Appl. Mech. Rev*. **2002**, *55* (6), 495-533.

[5] Ge, M.; Sattler, K. Bundles of carbon nanotubes generated by vapor-phase growth. *Appl. Phys. Lett*. **1994**, *64* (6), 710-711.

[6] Kiang, C.H.; Endo, M.; Ajayan, P.M.; Dresselhaus, G.; Dresselhaus, M.S. Size effects in carbon nanotubes. *Phys. Rev. Lett.*, **1998**, *81* (9) 1869–1872.

[7] Kis, A.; Zettl, A. Nanomechanics of carbon nanotubes. *Phil. Trans. R. Soc. A*, **2008**, *366*, 1591–1611.

[8] Endo, M.; Hayashi, T.; Kim, Y.-A. Large-scale production of carbon nanotubes and their applications. *Pure Appl. Chem.*, **2006**, *78* (9), 1703–1713.
[9] Ren, W.C.; Li, F.; Chen, J.; Bai, S.; Cheng, H.M. Morphology, diameter distribution and Raman scattering measurements of double-walled carbon nanotubes synthesized by catalytic decomposition of methane. *Chem. Phys. Lett*. **2002**, *359*, 196-202.
[10] Cirillo, G.; Hampel, S.; Spizzirri, U.G.; Parisi, O.I.; Picci, N.; Iemma, F. Carbon Nanotubes Hybrid Hydrogels in Drug Delivery: a perspective review. *BioMed Research International*, **2014**, Volume *2014*, Article ID 825017, 17 pp.
[11] Klumpp, C.; Kostarelos, K.; Prato, M.; Bianco, A. Functionalized carbon nanotubes as emerging nanovectors for the delivery of therapeutics. *Biochimica et Biophysica Acta*, **2006**, *1758*, 404 – 412.
[12] Sun, X.; Zeiger, H.J.; Kiang, C.-H.; Dresselhaus, M.S.; Endo, M. Model for interlayer spacing of multiwall carbon nanotubes. http://acs.omnibooksonline.com/data/papers/1997_ii386.pdf, pp. 386-387.
[13] Ajayan, P.M.; Zhou, O.Z. Applications of Carbon Nanotubes. In: Dresselhaus, M.S.; Dresselhaus, G.; Avouris, Ph. (Eds.). *Carbon Nanotubes, Topics Appl. Phys.* Springer-Verlag Berlin Heidelberg, **2001**, *80*, 391–425.
[14] Wong, C.H.; Vijayaraghavan, V. Nanomechanics of Nonideal Single- and Double-Walled Carbon Nanotubes. *J. Nanomater*. **2012**, Volume *2012*, Article ID 490872, 9 pp.
[15] Zhang, H.W.; Wang, L.; Wang, J.B. Computer simulation of buckling behavior of double-walled carbon nanotubes with abnormal interlayer distances. *Computational Materials Science*, **2007**, *39* (3), 664–672.
[16] Li., F.; Chou, S.G.; Ren, W.; Gardecki, J.A.; Harrison, G.R.; Swan, A.K.; Unlu, M.S.; Goldberg, B.B.; Cheng, H.-M.; Dresselhaus, M.S. Identification of the constituents of double-walled carbon nanotubes using Raman spectra taken with different laser-excitation energies. *J. Mater. Res*., **2003**, *18* (5), 1251-1258.
[17] Song, H.-Y.; Li, L.-F.; Feng, F. Torsional behaviour of carbon nanotubes with abnormal interlayer distances. *J. Phys. D: Appl. Phys.* **2009**, *42*, 055414, 5 pp. doi:10.1088/0022-3727/42/5/055414.
[18] Bichoutskaia, E.; Heggie, M.I.; Popov, A.M.; Lozovik, Yu.E. Interwall interaction and elastic properties of carbon nanotubes. *Phys. Rev. B*., **2006**, *73*, 045435.
[19] Huang, X.; Liang, W.; Zhang, S. Radial corrugations of multi-walled carbon nanotubes driven by inter-wall nonbonding interactions. *Nanoscale Res. Lett*. **2011**, *6* (53), 6 pp.
[20] Vukovic, T.; Damnjanovic, M.; Milosevic, I. Interaction between layers of the multi-wall carbon nanotubes. *Physica E*, **2003**, *16* (2), 259–268.
[21] Kuang, Y.D.; Shi, S.Q.; Chan, P.K.L.; Chen, C.Y. The effect of intertube van der Waals interaction on the stability of pristine and functionalized carbon nanotubes under compression. *Nanotechnology*, **2010**, *21*, 125704, 6 pp., doi:10.1088/0957-4484/21/12/125704.
[22] Su, W.S.; Leung, T.C.; Chan, C.T. Work function of single-walled and multi-walled carbon nanotubes: first-principles study. *Phys. Rev. B*, **2007**, *76*, 235413.
[23] Popov, A.M.; Lozovik, Yu.E.; Bichoutskaia, E.; Ivanchenko, G.S.; Lebedev, N.G.; Krivorotov, E.K. An Electromechanical Nanothermometer Based on Thermal Vibrations of Carbon Nanotube Walls. *Physics of the Solid State*, **2009**, *51* (6), 1306–1314.
[24] Wei, J.; Jiang, B.; Zhang, X.; Zhu, H.; Wu, D. Raman study on double-walled carbon nanotubes. *Chem. Phys. Lett*., **2003**, *376*, 753–757.

[25] Singh, D.K.; Iyer, P.K.; Giri, P.K. Diameter dependence of interwall separation and strain in multiwalled carbon nanotubes probed by X-ray diffraction and Raman scattering studies. *Diamond & Related Materials*, **2010**, *19*, 1281–1288.
[26] Pawlyta, M.; Łukowiec, D.; Dobrzańska-Danikiewicz, A.D. Characterisation of carbon nanotubes decorated with platinum nanoparticles. *Journal of Achievements in Materials and Manufacturing Engineering*, **2012**, *53* (2), 67-75.
[27] Dore, J.; Burian, A.; Tomita, S. Structural studies of carbon nanotubes and related materials by neutron and X-ray diffraction. *Acta Phys. Pol.*, **2000**, *98* (5), 495-504.
[28] Malesevic, A.; Kemps, R.; Zhang, L.; Erni, R.; Van Tendeloo, G.; Van Haesendonck, C. A versatile plasma tool for the synthesis of carbon nanotubes and few-layer graphene sheets. *J. Optoelectron. Adv. Mater.*, **2008**, *10* (8), 2052–2055.
[29] Yi, W.; Lu, L.; Pan, Z.W.; Xie, S.S. Linear specific heat of carbon nanotubes. *Phys. Rev. B.*, **1999**, *59* (14), R9015.
[30] Butko, V.Y.; Fokina, A.V.; Nevedomskya, V.N.; Kumzerov, Y.A. A template method for carbon nanotube production from sugar water. Cornell University Library, **2013**, arXiv:1309.3316, http://arxiv.org/abs/1309.3316.
[31] Ye, H.; Naguib, N.; Gogotsi, Yu. TEM Study of Water in Carbon Nanotubes. *JEOL News*, **2004**, *39* (2), 2-7.
[32] Gogotsi, Y.; Naguib, N.; Libera, J.A. *In situ* chemical experiments in carbon nanotubes. *Chemical Physics Letters*, **2002**, 365, 354–360.
[33] Zhou, O.; Gao, B.; Bower, C.; Fleming, L.; Shimoda, H. Structure and Electrochemical Properties of Carbon Nanotube Intercalation Compounds. *Molecular Crystals and Liquid Crystals*, **2000**, *340*, 541-546.
[34] Zhou, O.; Shimoda, H.; Gao, B.; Oh, S.; Fleming, L.; Yue, G. Materials Science of Carbon Nanotubes: Fabrication, Integration, and Properties of Macroscopic Structures of Carbon Nanotubes. *Acc. Chem. Res*. **2002**, **35**, 1045-1053.
[35] Mordkovich, V.Z.; Baxendale, M.; Yudasaka, M.; Kikuchi, R.; Yoshimura, S.; Dai, J.-Y.; Chang, R.P.H. In: Yoshimura, S.; Chang, R.P.H. (Eds.), Supercarbon: Synthesis, Properties and Applications, Springer, Berlin, **1998**.
[36] Colomer, J.-F.; Henrard, L.; Van Tendeloo, G.; Lucas, A.; Lambin, P. Study of the packing of double-walled carbon nanotubes into bundles by transmission electron microscopy and electron diffraction. *J. Mater. Chem*. **2004**, *14*, 603–606.
[37] Yoon, M.; Howe, J.; Tibbets, G.; Eres, G.; Zhang, Z. Polygonization and anomalous graphene interlayer spacing of multi-walled carbon nanofibers. *Phys. Rev. B.*, **2007**, *75*, 165402, 6pp.
[38] Wu, F.Y.; Cheng, H.M. Structure and thermal expansion of multi-walled carbon nanotubes before and after high temperature treatment. J. *Phys. D: Appl. Phys*. **2005**, *38*, 4302–4307.
[39] Howe, J. Y.; Tibbetts, G. G.; Kwag, C.; Lake, M.L. Heat treating carbon nanofibers for optimal composite performance. *J. Mater. Res*. **2006**, *21*, 2646-2652.
[40] Crespi, V.H.; Chopra, N.G.; Cohen, M.L.; Zettl, A.; Louie, S.G. Anisotropic electron-beam damage and the collapse of carbon nanotubes. *Phys. Rev. B.*, **1996**, *54* (8), 5927-5931.
[41] Xu, Z.; Chen, L.; Liu, L.; Wu, X.; Chen, L. Structural changes in multi-walled carbon nanotubes caused by γ-ray irradiation. *Carbon*, **2011**, *49*, 339-351.
[42] Salonen, E.; Krasheninnikov, A.V.; Nordlund, K. Ion-irradiation-induced defects in bundles of carbon nanotubes. *Nuclear Instruments and Methods in Physics Research B*, **2002**, *193*, 603–608.

[43] An, K.H.; Heo, J.G.; Jeon, K.G.; Bae, D.J.; Jo, C.; Yang, C.W.; Park, C.-Y.; Lee, Y.H. (2002) X-ray photoemission spectroscopy study of fluorinated single-walled carbon nanotubes. *Appl. Phys. Lett*., **2002**, *80*, 4235–4237.

[44] Wepasnick, K.A.; Smith, B.A.; Bitter, J.L.; Howard Fairbrother, D. Chemical and structural characterization of carbon nanotube surfaces. *Anal. Bioanal. Chem*. **2010**, *396* (3), 1003-1014.

[45] Golovaty, D.; Talbott, S. Polygonization of carbon nanotubes. **2013**, http://xxx.tau.ac.il/pdf/0711.1719.pdf.

[46] Golovaty, D.; Talbott, S. Continuum model of polygonization of carbon nanotubes. *Phys. Rev. B*, **2008**, *77*, 081406.

[47] Behler, K.; Osswald, S.; Ye, H.; Dimovski, S.; Gogotsi, Yu. Effect of thermal treatment on the structure of multi-walled carbon nanotubes. *Journal of Nanoparticle Research*, **2006**, *8*, 615–625.

[48] Hod, O. Graphite and Hexagonal Boron-Nitride have the Same Interlayer Distance. Why? *J. Chem. Theory Comput*. **2012**, *8*, 1360−1369.